Journal Home Page: https://sites.google.com/a/univsul.edu.iq/sjes

Review Article:

Direct shear strengthening of NSC and SCC using NSM CFRP and steel bars

Rozhno Omer Mustafa[1]
Mohamed Raouf Abdul-Kadir[1]

[1]University of Sulaimani, College of Engineering, Civil Engineering Department.

Article Inform

Article History:
Received 8 July 2019
Accepted 28 August 2019
Available online 1 June 2020

Keywords: Direct shear, NSM, Strengthening, CFRP rod.

About the Authors:
Corresponding author:
Rozhno Omer Mustafa - MSc.
E-mail: rozhnw.mustafa@univsul.edu.iq
Researcher Involved:
Dr. Mohamed Raouf Abdul-Kadir - Professor.

DOI Link: https://doi.org/10.17656/sjes.10126

Abstract

Failure in direct shear is sudden and catastrophic in concrete structures, Several techniques have been developed for shear strengthening of push-off specimens representing direct shear. In this research, the effectiveness of Near-surface mounted (NSM) FRP and steel bars as a strengthening technique for direct shear in normal strength concrete (NSC) and self-compacted concrete (SCC) are studied. As a result of the experimental work, it was observed that the NSM steel bars increased the shear capacity by 48 and 44% for both types of concrete NSC and SCC respectively, while the NSM CFRP rods increased the shear capacity by 30% and 33% for both NSC and SCC respectively. It was also observed that strengthening at 90° was more effective in terms of shear strength compared to 45° with a difference in the range of 8% for NSC and 5% for SCC. The analytical results are very close to the experimental ones.

1. Introduction

Employment of fiber reinforced polymer (FRP) composites to repair and retrofit concrete elements has been steadily increasing. The use of near surface mounted (NSM) fiber reinforced polymer (FRP) rods is a promising technology for increasing flexural and shear strength of deficient reinforced concrete members. Design of members for direct shear is usually made using shear friction method, which is accepted by the (ACI 318-14). If cracks occur in members subjected to direct shear there is a need for strengthening to avoid complete collapse.

Saenz N. et al. (2005) tested thirty-six internally unreinforced push-off specimens cast using

concrete with $f'_c = (34 - 37)$ MPa. They used CFRP laminate for strengthening in three groups and four CFRP ratios of 0.31%, 0.62%, 0.82% and 1.23%. The average shear load enhancement was 74.86%, 66.75%, 67.67% and 65.2% for the four ratios, respectively. They observed that the three strips of CFRP (with the same CFRP ratio) provided greater load enhancement compared to the other wrapping scheme. The shear friction strength of un-cracked concrete externally reinforced with CFRP composites ranged from 0.17 f'_c to 0.27 f'_c.

Zangana B. A. M. (2008) tested 27 unreinforced push-off specimens, with average f'_c of 34 MPa. The specimens of the first group were strengthened with one, two and three layers of GFRP at 90° and 45°. The same number of specimens in another group were strengthened using CFRP laminate. For 45° inclined strips the shear strength performance of GFRP was better than that of CFRP. The strengthened specimen with CFRP at 90° provided more shear strength compared to those specimens strengthened with the same CFRP strips at 45°. He concluded that CFRP strips had more significant contribution on shear strength enhancement compared to GFRP strips.

Jayaprakash J. et al. (2009) investigated the shear transfer capacity and mode of failure of reinforced concrete pre-cracked push-off specimens bonded externally with a layer of bi-directional CFRP sheets. The shear reinforcements ratio provided across the shear plane were (0.14%, 0.28% and 0.42%) and a concrete with $f'_c = 30$ MPa was used. They concluded that when the internal shear reinforcement increased, the contribution of CFRP laminate on the shear enhancement is reduced. The results indicated that shear displacement was significantly low for strengthened specimens, but there was a sudden increase in a shear slip at the peak load.

Shariatmadar H. et al. (2013) conducted tests on six pre-cracked push-off concrete specimens with $f'_c = 37$ MPa. The specimens were divided into two groups both with ρ_v = (0.92%, 1.23% and 1.54%). One group was not strengthened but the other was strengthened externally with two layers of 140 mm wide CFRP strips (ρ_f = 0.35%). The shear strength was increased by 5.24% for the specimens strengthened with two layers CFRP strips. The contribution of CFRP laminate on the shear strength reduces when the amount of internal steel reinforcement increases.

Naserian R. et al. (2013) study included testing of 16 non-cracked push-off specimens internally reinforced with steel reinforcement with ratios between zero and 1.54% and externally strengthened with different widths of Glass FRP layers (0,90,140 and 240 mm). In the strengthened specimens, shear transfer capacity increased from 3% to 38% compared to non-strengthened specimens. The contribution of FRP reinforcement in shear transfer capacity, as the percentage of cylindrical concrete strength (f'_c), was between 0.6% f'_c and 3.7% f'_c.

Fattah O. A. (2016) conducted tests on twenty push-off specimens with (0, 0.0067, 0.01 and, 0.0134) shear reinforcement ratio. The strengthening was made with one or two layers of CFRP. The test results showed that the contribution of CFRP laminates and their ratio were more effective for non-reinforced concrete compared to reinforced concrete subjected to direct shear. The shear strength enhancement compared to control specimens were 1.91, 1.29, 1.18 and 1.17 for the four shear reinforcement ratios respectively.

2. Research objectives

The main objectives of this research are to study shear strength modes of failure and deformation behavior of push off specimens subjected to direct shear after strengthening using different materials and methods, focusing on the NSM technique with FRP and steel bar applied in

different configurations. The techniques are applied on two types of concrete with similar compressive strength namely NSC and SCC.

3. Materials and Experimental Work

3.1 Experimental Program

Twenty push- off concrete specimens with the same shear reinforcement ratio of ρ_v = 0.013 were tested, with dimensions as shown in Fig.1. The specimens were classified into two group, with ten specimens each, the first group was cast with normal strength concrete (NSC) and the second group was self-compacted concrete (SCC). Then each group is classified as control, strengthened with CFRP rod and strengthened with steel bar as summarized in Table 1.

3.2. Materials

The materials used in experimental works were necessary to prepare normal strength concrete (NSC) mix and self-compacted concrete (SCC) mix with a designed cylinder compressive strength of 50 MPa using Ordinary Portland Cement (Type I) from Tasluja company. Natural sand from Darbandikhan area was used as fine aggregate with grading conforming to (ASTM C136, 2014) with specific gravity = 2.64. Natural gravels from Goptapa region with nominal maximum size (19 mm) was used for the NSC, however, course aggregate grade of (Max. size Agg. =12.5 mm) was used for the self-compacting concrete. Deformed steel bars of Ø 8 mm diameter with $f_y = 384$ MPa and $f_u = 531$ MPa was used as shear reinforcement and for strengthening purposes, steel bar of Ø 16 mm with $f_y = 522$ MPa and $f_u = 648$ MPa was used for L-shaped parts of push-off specimens.

High-Performance Superplasticizer admixture was used in the production SCC mix to improve workability and increase ultimate strength. The external strengthening material was carbon fiber reinforced polymer (CFRP) rebar with tensile strength $f_u = 2000$ MPa was used with adhesive epoxy resin (Sikadur-330) to place CFRP rods in the groove of the concrete surface for the NSM technique.

The properties of the concrete are summarized in Table 2. The mix proportions of SCC satisfy the criteria of filling ability and segregation resistance, specified by L-box, V-funnel and slump flow. These tests were conducted to ensure the suitability of the mix. The testing apparatus is shown in Figure 2 and the results are shown in Table 3 (EFNARC Guidelines., 2005).

3.3. Specimen Preparation

The molds for the specimens were designed to be erected easily and made of two parts from the galvanized steel plate of 3 mm thickness. The two parts were connected with screws and bolts in two opposite corners. The specimen mold was connected tightly to a plywood base using fast screws. The materials for each batch were prepared by weight, then mixed in an electrical tilting mixer of (0.08 m^3) capacity. The mixing operation was continued until workable concrete was obtained.

The concrete was then poured into the forms with the steel cage inside in two-layer and each layer for (NSC) was vibrated for about 30 seconds. Along with each group, six cylinders (300 mm * 150 mm) were cast as a control for compressive strength of concrete and six cylinders (200mm*100mm) were cast for splitting tensile strength of concrete.

3.4. Strengthening process with CFRP rod and steel bar using NSM technique

The following steps were carried out during strengthening process:

On the surface of the concrete, grooves were cut by hand cutting and hammer drilling machine

after marking the layout. The grooves were cleaned and brushed dust free before working on it, the epoxy resin mixture was applied and half-filled the grooves. The CFRP rod or steel bar was placed inside the groove and pressed lightly to be fixed, then the groove was filled with resin and the surface was leveled. The grooves on the surface were cut at 90° angle (perpendicular to the shear crack plane) and at 45° angle for strengthening the specimens as shown in fig. 3.

3.5. Testing procedure

All specimens were tested under a single point loading. Loading was applied through a controlled hydraulic operated jacking with a maximum capacity of (700 kN), fixed to the loading frame as shown in Fig.4. the instrumentation was so arranged to apply the load at the center of the specimen without eccentricity and to prevent local failure. The load was applied gradually with 10 kN increments till failure at the shear plane.

The vertical displacement which represents the slip along the shear plane and the lateral displacement that represent the cracking width in the push-off specimens were measured using three linear variable displacement transducer (LVDT) with (0.001 mm) precision, two at the front for indicating the crack width and one for the slip in the other sides of the specimen. Electrical resistance strain gauges of (0.01 mm) accuracy with P-3500 digital strain indicator were used to measure the tensile strain in the steel and CFRP rods and compression strain in the concrete. The control cylinder specimens were tested using the compression testing machine of 3000 kN capacity.

4. Results and Discussion

Results of concrete compressive strength obtained from the control cylinder specimens, the ultimate and first crack load, shear strength, first crack load ratio (strengthened/control) and shear strength ratio (strengthened/control) for all the tested push-off specimens are presented in Table 4.

4.1. Behavior of the Push-off specimen

A comparison is made between the control specimen and the strengthened ones for each group in terms of mode of failure, cracking and ultimate loads, displacement and strain.

4.1.1. Modes of failure

As loads were applied gradually, the shear cracks appeared near the shear plane and by increasing loads the cracks propagated toward the center of the shear plane. Failure in the control specimens (C1 and D1) initiated with cracks occurred at both sides along the shear plane, these cracks extended and well-observed until reaching failure load. Even though cracking occurred, the L-shaped parts of the push-off specimens did not split completely because of the presence of shear reinforcement across the shear plane. However, at the final failure of the specimen the L-shaped parts split apart without rupture of the shear reinforcement as shown in Fig.5.

For the remaining specimens, the failure of the specimens strengthened at both 45° and 90° initiated at the strengthening area at the same angle of the bars at the weakest point (between bars). The final failure was debonding of the bars by splitting of the concrete cover and cracking of the surrounding concrete, associated with the diagonal tension failure of concrete. This mode of failure was more obvious in the specimens strengthened at 90° angle as shown in Figs. 6 and 7. This type of failure may be prevented by providing better anchorage of the NSM bars crossing the critical shear crack, either by anchoring the bars into the concrete shear plane

or using bars fully wrapped bars around the specimen.

4.1.2. Cracking and ultimate loads

Reforming to Table 4, the results show that the presence of NSM CFRP and steel bars increases the first cracking load. The ratio of cracking shear strength of CFRP strengthened specimens to control specimens are 1.12 and 1.36 for NSC for C2 and C3 respectively, and for SCC the values 1.06 and 1.24 for D2 and D3 respectively, however, for the steel strengthened specimens the ratios are 1.36 and 1.49 for NSC for C4 and C5 respectively, and 1.12 and 1.41 for SCC for D4 and D5 respectively. The cracking ratios in strengthened steel bar specimens are higher compared to CFRP specimens.

In the internally reinforced specimens when cracking initiates along the shear plane, the shear reinforcement provided across the crack support the extra shear stresses as clamping force till the steel reinforcement yields. As seen from Table 4, for normal strength concrete specimens (Group C), the ratio of shear strength after strengthening with CFRP rods at 45° and 90° (C2 and C3) were 1.26 and 1.36 respectively. However, the shear strength ratios were equal to 1.43 and 1.52 for steel bar strengthening at 45° and 90° respectively. For the self-compacted concrete group D specimens, the shear strength of the specimen strengthened with CFRP rods compared to D1 have increased by 1.30 and 1.35 for (D2 and D3) for 45° and 90° inclinations respectively. For specimens D4 and D5 strengthened with steel bars the increments were 1.40 and 1.47 times the control D1. This indicates that the steel bars were performing better than CFRP bars for both inclination arrangements and for both types of concrete. The ultimate shear strength in SCC (group D) is higher than in NSC (group C) due to the high tensile strength in SCC. Although the shear strength enhancement is moderate, the process of strengthening concrete using CFRP rod or steel bar is acceptable.

4.2. Deformation characteristics

4.2.1. Slip

At the beginning of cracking the slip between the two halves of the specimen as measured by the vertical LVDT occurred as a result of the compression of the inclined concrete struts between reinforcement crossing the shear plane. The component of this compression parallel to the shear plane is referred to slipping when discussing its behavior.

Fig.8 shows the shear stress - slip relationship of the specimens strengthened with different strengthening materials and angle of configuration. It is noticed that strengthening with steel bars at 90° (C5 and D5) reduced the amount of the slip in the specimens more than other specimens at same stress value for both NSC and SCC, the reason may be due to effect of strengthening technique inclination. Figure 9 shows the slip at failure for Group C and Group D. The figure shows that the slip at failure in group C (NSC) specimens is lower than that in Group D (SCC) specimens. Hence Group C showed an increase in stiffness, but failed in a brittle manner.

4.2.2. Crack width

The shear stress and crack width relationship of the strengthened and un-strengthened specimens are shown in Fig. (10). The figures show that the strengthened specimens showed a smaller value of shear displacement and crack width at failure load compared to un-strengthened specimens. The specimens with bars placed at 90° angle such as C3, C5, D3, and D5 exhibited less crack width compared to other specimens because the bars are perpendicular to the cracks. Fig.11 shows Crack width at failure for Group C and Group D specimens, the figure shows that group D specimens exhibited

low crack width compared to group C, this may be because in normal strength concrete (Type C) the bond strength between mortar and aggregate particles is low, cracks generally propagate around the aggregate particles, producing a rough surface, while in Self-compacted concrete (Type D) the bond strength between mortar and aggregate particles is apparently greater, as indicated by the splitting tensile strength for NSC and SCC are (4.67 and 5.16 MPa) respectively.

4.2.3. Strain in concrete, steel and CFRP bars

The maximum compression strain of concrete at the surface of the shear plane terminates at the end of loading. It should be noted that this strain is related to clamping stress. Fig.12 shows the shear stress relationship with a concrete strain of the un-strengthened and strengthened specimens. It is noticed that the concrete strengthened with a steel bar at 45° has the maximum strain amount compared to all of the other specimens for both NSC and SCC. Fig.13 shows the comparison of concrete strain for group C (NSC) and group D (SCC) specimens. It can be noticed that the strain for both groups is too close with a small difference which is higher in group D at the same load especially at large shear stresses.

Fig.14 show the results of tensile strain in the stirrups for the strengthened specimens. The figure shows that the strain in stirrups in strengthened specimens is much smaller than in non-strengthened specimens. This may be the effect of the strengthening technique which reduces load transfer to the stirrups, and shear reinforcement dowel action is minimized in contrary to non-strengthened specimens. Fig.15 shows the shear stress-strain in stirrups relationship for Group C and Group D, which shows that internal shear reinforcement strains in both NSC and SCC are the same until reaching high shear stress at which group D exhibit higher strains in their stirrups due to the high shear strength of this

The shear stress-strain for strengthening materials in group C and D specimens are shown in Fig. (16). After concrete cracking, the steel and CFRP rods are strained. However, after their peak shear stress is reached, the strengthening materials debonded rapidly and consequently, the strain dropped. Based on the results, strain in steel bar was smaller than that in the CFRP rod, due to a higher bond between the deformed steel bars and epoxy resin the NSM technique.

The strain in steel bars for group C (NSC) was approaching yield strain. Fig. (17) shows the shear stress–strain relationship for strengthening materials in Group C and Group D, the figure shows that group D (SCC) specimens exhibited low strain compared to group C (NSC), this may be due to the high tensile strength in SCC.

5. Theoretical analysis

In this section some of present models for shear strength prediction are presented and from the data collected from tests and using regression analysis a new model for direct shear strength of concrete strengthened with NSM technique is proposed.

5.1. Present models for direct shear strength prediction

Mattock, A. H. (2001) proposed simple equations for shear friction design, which allow the full potential shear transfer strength of concrete to be utilized. This equation is expressed as follows:

$$v_n = 0.1\, f'_c + 0.8\, \rho_v f_y \qquad \text{Eq. (1)}$$

Where f'_c is concrete strength and not more than 55 MPa, f_y = yield stress of shear friction reinforcement and ρ_v = internal reinforcement ratio.

Saenz N. et al. (2005) presented an equation to determine the concrete shear friction strength and the additional shear friction strength provided by the concrete–CFRP interaction, the relation between ultimate shear to concrete compressive strength, v_u/fc' versus effective CFRP composite tensile stress normalized by the concrete compressive strength is calculated and the line of best fit is

$$v_u = 0.117\, fc' + 0.505\, \rho_f f^* f_u \qquad \text{Eq.(2)}$$

Where $\rho_f f^* f_u$ is the effective CFRP composite tensile stress, which is the clamping stress provided by the CFRP composite.

Mohammed A. A. et al. (2012) for the case of unidirectional CFRP laminate obtained the following equation from regression analysis for the shear enhancement of plain concrete after strengthening.

$$\Delta_{vn} = 0.069\left(\rho_f f_f + \rho_{fi} f_{fi} cos\alpha\right)^{1.177} \qquad \text{Eq.(3)}$$

In which Δ_{vn} is the shear strength enhancement, ρ_f is the ratio of CFRP layer in the concrete section perpendicular to the shear plane, f_f is the fracture tensile stress in CFRP material, ρ_{fi} is the CFRP ratio of the inclined strips provided to the section and α is the angle of inclined strips measured from shear plane, and f_{fi} is the fracture tensile stress of the lettered CFRP laminate. The shear strength of strengthened concrete is that of plain concrete plus that obtained from the value obtained from the above equation multiplied by the basic shear strength.

Naserian R. et al. (2013) obtained three equations for calculating direct shear strength of non-cracked concrete strengthened with GFRP laminate, for three steel reinforcement parameter ($\rho v\ fy$) equal to 3.3, 4.4 and 5.5 MPa. Later, a refined equation for all reinforcement ratios having the following form was obtained from a regression analysis

$$v_u = 0.116\, f'_c + 0.803\, \rho_v f_y + 0.144\, \rho_f f_{fu} \qquad \text{Eq.(4)}$$

Where ρ_f = external reinforcement ratio, f_{fu} = ultimate tensile strength of FRP strip.

Fattah O. A. (2016) proposed equation for shear strength for plain and reinforced concrete, strengthened with CFRP laminate or GFRP laminate based on 20 specimen which were classified into four groups, according to shear reinforcement ρυ (0, 0.0067, 0.01, and 0.0134. After regression analysis the final equation for the shear strength was

$$v_n = 0.132\, f'_c + 0.636\, \rho_v f_y + 0.389\, \rho_f f_{fu^*} \qquad \text{Eq.(5)}$$

In which ρ_f = external reinforcement ratio, f_{fu^*} is the composite tensile strength of the laminate.

5.2. Prediction of Direct Shear Strength of Concrete with NSM bars

Based on the properties of concretes with different type of strengthening materials and degree of orientation for strengthening technique, an equation is proposed for shear strength of concrete strengthened with NSM bars. Since type of concrete and degree of bar inclinations are different in each group, the shear transfer capacity is computed by adding another term to consider the contribution of FRP rod (v_f) and external steel bar (v_{se}). This equation is expressed as following:

$$v_u = a^*\left(b\, fc' + c\, \rho_v f_y + d\, \rho_f f_{fu} * \sin\alpha + e\, \rho_v f_{su} * \sin\alpha\right) \qquad \text{Eq.(6)}$$

Where: a^* = coefficient for type of concrete (NSC and SCC), b = concrete cohesion coefficient; c = concrete–stirrup shear friction interaction

coefficient; d = concrete–FRP shear friction interaction coefficient; e = concrete–external steel bar shear friction interaction coefficient; α = degree of inclination strengthening material in NSM technique (45° and 90°); f_{fu} = ultimate tensile strength of the CFRP rod; f_{su} = ultimate tensile strength of the steel bar. A linear regression analysis was used for the test results and the final equation for the direct shear strength is :

$$v_u = a^* (0.120\, fc' + 0.800\, \rho_v f_y + 0.757\, \rho_f f_{fe} * \sin\alpha + 2.106\, \rho_v f_{se} * \sin\alpha) \quad \text{Eq.(7)}$$

Where : $a^* = 1\ for\ NSC\ and\ \ a^* = 1.081\ for\ SCC$

The correlation coefficient (R^2) for the above relationship is 0.95 while the mean value (test / predicted) is 1.01 and standard deviation is 0.25 as shown in Fig.18. These values indicate that there is a valid agreement between the test results and the predicted shear strength. When this equation is applied to result of past models (Mattock, A. H., 2001, and others), and including this research, the mean (test / calculated) shear strength based on the proposed equation is equal to 0.90, and standard deviation is 0.33 as shown in Fig.19.

6. Conclusions

Based on the experimental and analytical investigations, the following main conclusions can be drawn:

- NSM strengthening technique with CFRP bars (6 mm diameter) for reinforced push-off specimens increase the shear strength capacity by 1.31 and 1.33 for NSC, and SCC respectively.
- The increments for the NSM steel bars with (8 mm diameter) were 1.48 and 1.44. The NSM technique was more effective for steel bars.
- The ultimate shear load capacity increment for shear strengthening in NSC is a little higher than in SCC when using the same strengthening techniques.
- The strengthening by CFRP rods and steel bars at a 90° angle were more effective in terms of maximum load-carrying capacity compared to 45° angle, the difference was in the range of % 8 for NSC and % 5 for SCC in reinforced specimens.
- The conventional steel bars strengthened specimens showed a slightly more favorable response than those strengthened with CFRP rod to direct shear strength by 1.13 for NSC and 1.09 for SCC specimens.
- In the un-strengthened specimens, the cracks occurred along the shear plane until reaching failure load. However, for the strengthened specimens, the failure occurred at the same angle of strengthening rods at the weakest region (between rods) and debonding happened in all the specimens as indicated by stripping off the strengthened part.
- The shear displacement (shear slip) and crack width of the strengthened specimens were less compared to the un-strengthened specimens for the same load. However, there was a sudden increase as the load reaches its peak.
- At maximum load, the crack width in the NSC was 2.6 mm compared to 2.2 mm for SCC specimens.
- The maximum vertical displacements (shear slip) were 9.5 mm and 8.8 mm for NSC and SCC specimens respectively.
- The proposed model equation showed good results when applied to the experimental results of this investigation and others experimental results.

تقوية القص المباشر للخرسانة العادية والخرسانة ذاتية الرص باستخدام قضبان ألياف الكربون البوليمرية والحديد مثبتة قرب السطح

رۆژنۆ عمر مصطفى[1] - ماجستير
د. محمد رۆوف عبدالقادر[1] - استاذ

[1] جامعة السليمانية ، كلية الهندسة ، قسم الهندسة المدنية

المستخلص

الفشل عند قص المباشر للمباني الخرسانية يكون مفاجئا وخطراً. لقد تم تطوير العديد من طرق التقوية لنماذج تخص القص المباشر. الهدف من هذا البحث كان دراسة تأثير تقنية التقوية عن طريق وضع القضبان قريبة من سطح الخرسانة لنماذج من خرسانة العادية المقاومة والخرسانة ذاتية الرص. قد بينت نتائج الفحوصات بأن التقوية بقضبان ألياف الكربونية تزيد من مقاومة القص المباشر بنسبة 30% و 33% للخرسانة العادية وذاتية الرص على التوالي حيث كانت الزيادة 44% و 48% عند استعمال قضبان الحديد للتقوية. كما وإن استعمال تقنية NSM تقلل من عرض الشقوق و كمية الانزلاق والتشوه الحاصل في قضبان القص الداخلي. كما واظهرت النتائج بأن التقوية بزاوية 90 لكلا النوعين من القضبان العطت مقاومة قص اكبر من النماذج المقواة بزاوية 45 بنسب تتراوح من 8% الى 5% للخرسانة العادية والخرسانة ذاتية الرص على التوالي. التحليلية قريبة جدا من النتائج التجريبية.

الكلمات المفتاحية : القص المباشر ، NSM ، التقوية ، CFRP ، الخرسانة العادية ، الخرسانة ذاتية الرص.

References

1- American Concrete Institute. (2014). Building Code Requirements for Structural Concrete (ACI 318-14): Commentary on Building Code Requirements for Structural Concrete (ACI 318R-14): an ACI Report. American Concrete Institute. ACI.
2- ASTM C136. "Standard Test Method for Sieve Analysis of Fine and Coarse Aggregates.", Annual Book of ASTM Standard, Vol. 04, October 2014.
3- EFNARC Guidelines. (2005). The European Guidelines for Self-Compacting Concrete; Specification, Production and Use. p. 63.
4- Fattah, Omed Amin (2016). "Strengthening concrete for Direct Shear." MSc. thesis University of Sulaimani.
5- Jayaprakash, J., Samad, A. A. A., & Abbasvoch, A. A. (2009). Experimental Investigation on Shear Capacity of Reinforced Concrete Pre-cracked Push-off Specimens with Externally Bonded Bi-Directional Carbon Fiber Reinforced Polymer Fabrics. *Modern Applied Science*, *3*(7), 86-98.
6- Mattock, A. H. (2001). Shear friction and high-strength concrete. *Structural Journal*, *98*(1), 50-59.
7- Mohammed, A. A., & Hassan, G. B. (2012). Prediction of Load Capacity of Reinforced Concrete Corbels Strengthened with CFRP Sheets. *World Academy of Science, Engineering and Technology, International Journal of Civil, Environmental, Structural, Construction and Architectural Engineering*, *6*(8), 563-568.
8- Naserian, R., Hosseini, A., & Marefat, M. S. (2013). Assessment of shear transfer capacity of non-cracked concrete strengthened with external GFRP strips. *Construction and Building Materials*, *45*, 224-232.
9- Saenz, N., & Pantelides, C. P. (2005). Shear friction capacity of concrete with external carbon FRP strips. *Journal of structural engineering*, *131*(12), 1911-1919.
10- Shariatmadar, H., Khatamirad, M., & Zamani, E. (2013). Pre-cracked concrete shear strengthened with external CFRP strips. Journal of rehabilitation in civil engineering, 1(1), 29-38.
11- Zangana, Bakhtiar Aziz (2008). "Effect of wrapped R.C beams by carbon and glass Fiber strips internally and externally to the Shear Capacity." MSc. thesis University of Mosul.

Table 1: Details classification of push off specimen. (Source: Researcher)

Group		Type of concrete	Technique of strengthening	Strengthening material	Degree of inclination
C	C1	Normal Strength Concrete	Control	Not strengthening	---------
	C2		NSM	CFRP rode, 6 mm	45 °
	C3		NSM	CFRP rode 6 mm	90 °
	C4		NSM	Steel bar, 8 mm	45 °
	C5		NSM	Steel bar, 8 mm	90 °
D	D1	Self-Compacted Concrete	Control	Not strengthening	----------
	D2		NSM	CFRP rode, 6 mm	45 °
	D3		NSM	CFRP rode 6 mm	90 °
	D4		NSM	Steel bar, 8 mm	45 °
	D5		NSM	Steel bar, 8 mm	90 °

Table 2: Mix compositions of NSC and SCC. (Source: Researcher)

	Materials (Kg / m^3)							
Type of Concrete	Cement	Fine Agg.	Coarse Agg. Max. 19 mm	Coarse Agg. Max. 12.5 mm	Water	S.P	W / C	Mix Proportion C : S : G
Normal Strength Concrete (NSC)	500	870	1190	_____	210	0	0.42	1:1.74:2.38
Self-Compacted Concrete (SCC)	465	1380	_____	1000	158	6.32 (% 1.36)	0.34	1:2.97:2.15

Table 3: SCC properties requirements as per EFNRC 2005. (Source: Researcher)

Method	Results	Minimum Range	Maximum Range
Slump flow (mm)	690	550	850
T 500 mm Slump flow (sec.)	8	2	9
V-funnel (sec.)	11	6	12
L Box (h2 / h1)	0.81	0.7	1.0

Table 4: Test Results. (Source: Researcher)

Group	Specimen designation	f'_c (MPa)	Splitting Tensile Strength (f_{ct}) (MPa)	First crack load (kN)	Ultimate load (P_u) (kN)	Ultimate shear strength (v_u) (MPa)	First crack load ratio (strengthened / control)	Shear strength ratio (strengthened / control)
C	C1	53.73	4.67	290	342	11.40	-	-
	C2			324	432	14.40	1.12	1.26
	C3			396	468	15.60	1.36	1.36
	C4			396	490	16.33	1.36	1.43
	C5			432	522	17.40	1.49	1.52
D	D1	51.14	5.16	306	360	12.00	-	-
	D2			324	468	15.60	1.06	1.30
	D3			378	486	16.20	1.24	1.35
	D4			342	504	16.80	1.12	1.40
	D5			432	530	17.66	1.41	1.47

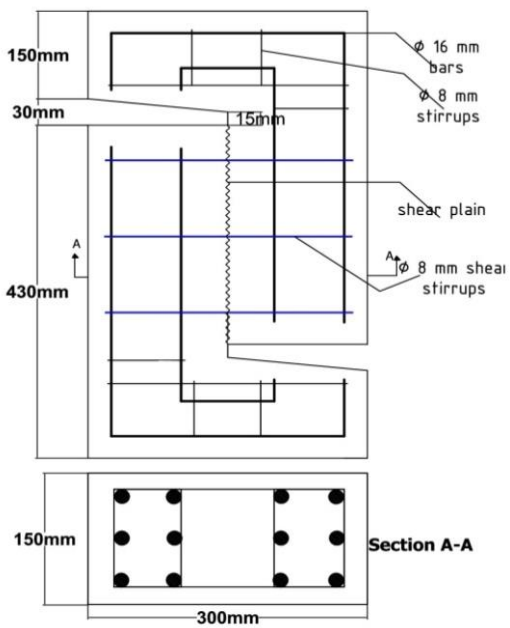

Fig.1: Detail of test specimen, ρυ = 0.013 , Aυ= 6 ø 8 mm bars. (Source: Researcher)

(a)

(b)

(c)

Fig. 2: Rheological parameters of the SCC: (a) Slump flow; (b) V-funnel; (c) L Box test (EFNARC Guidelines., 2005).

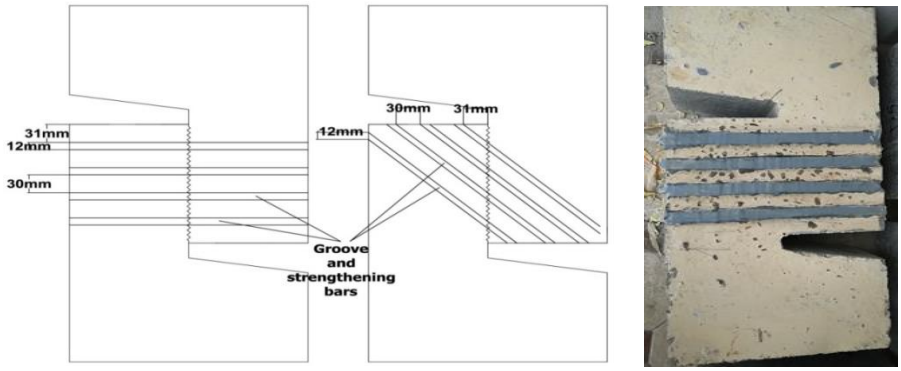

Fig. 3: Dimensions of the grooves for the strengthening bar and NSM technique. (Source: Researcher)

Fig. 4: Instrument and push off specimen that ready for test. (Source: Researcher)

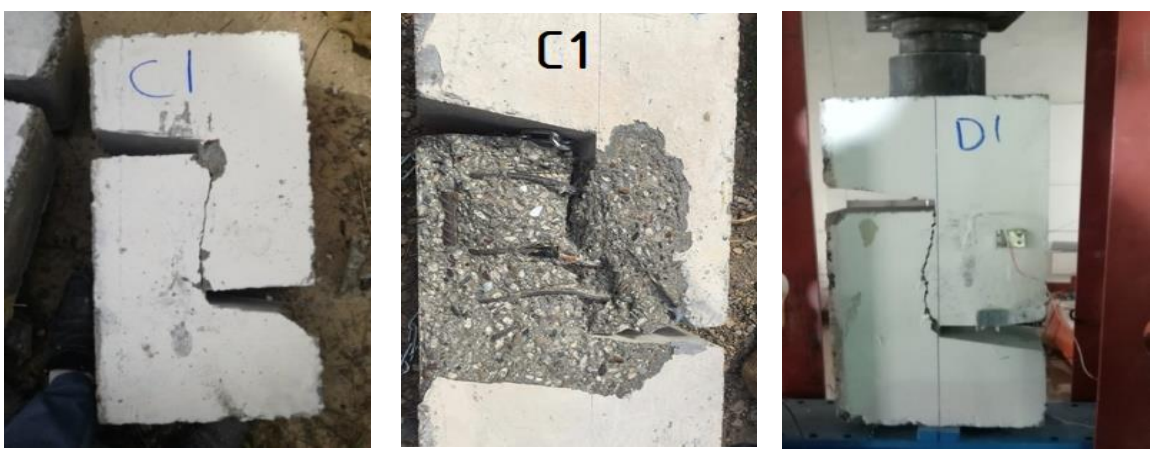

Fig. 5: Specimens C1 and D1 after failure. (Source: Researcher)

Fig. 6 : Specimens C2, D2, C4 and D4 after failure. (Source: Researcher)

Figure 7 : Specimens C3, D3, C5 and D5 after failure. (Source: Researcher)

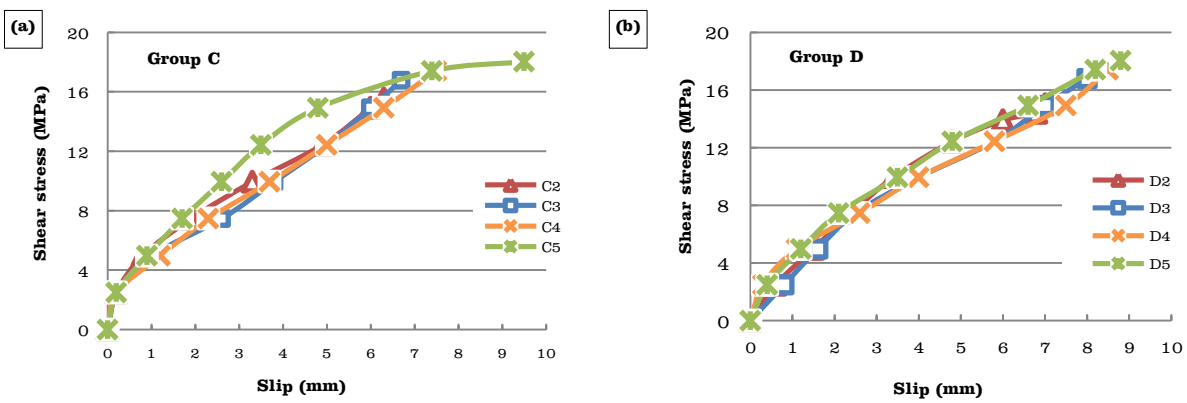

Fig. 8: Shear stress – vertical slip relationship: (a) Group C ; (b) Group D. (Source: Researcher)

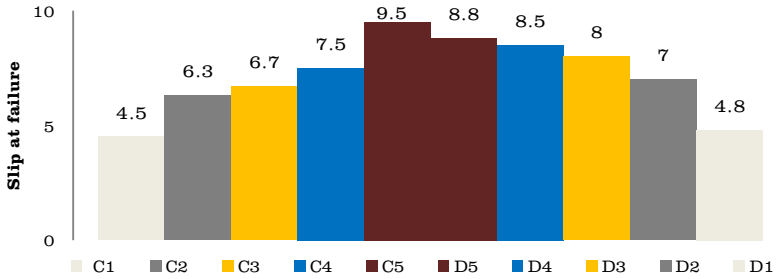

Fig. 9: Slip at failure for Group C and Group D. (Source: Researcher)

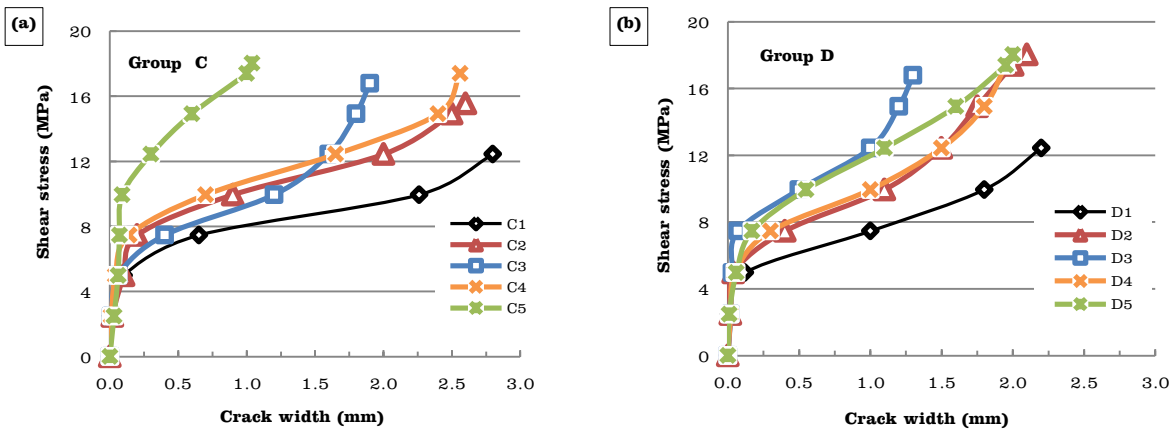

Fig.10: Comparison of Shear stress – Crack width relationship : (a) Group C ; (b) Group D . (Source: Researcher)

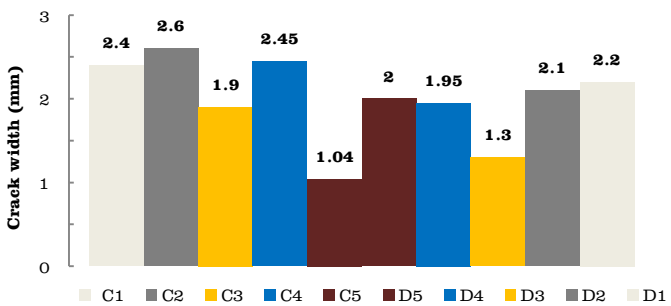

Fig. 11: Crack width at failure for Group C and Group D. (Source: Researcher)

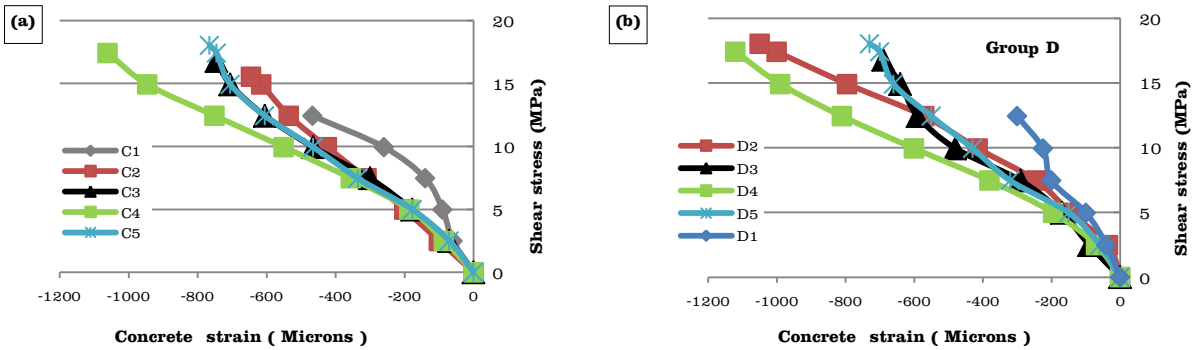

Fig. 12: Shear stress – Concrete strain relationships : (a) Group C ; (b) Group D. (Source: Researcher)

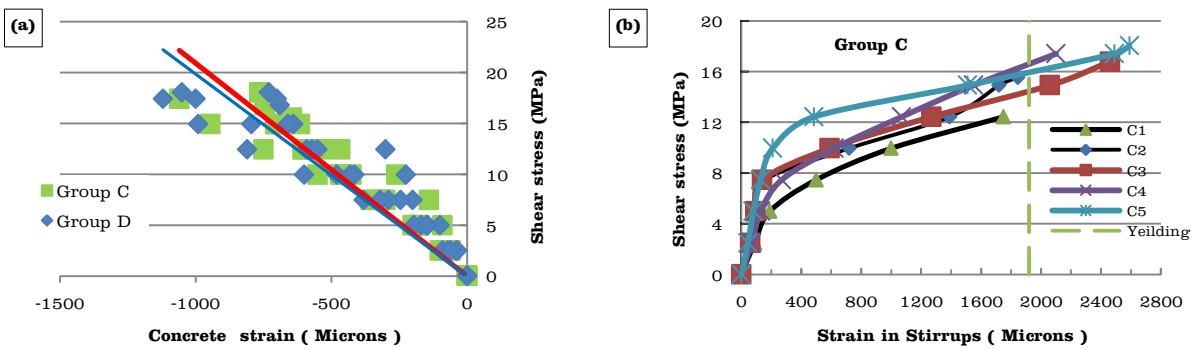

Fig. 13: Shear stress – Concrete strain relationship for Group C and Group D. (Source: Researcher)

(a)

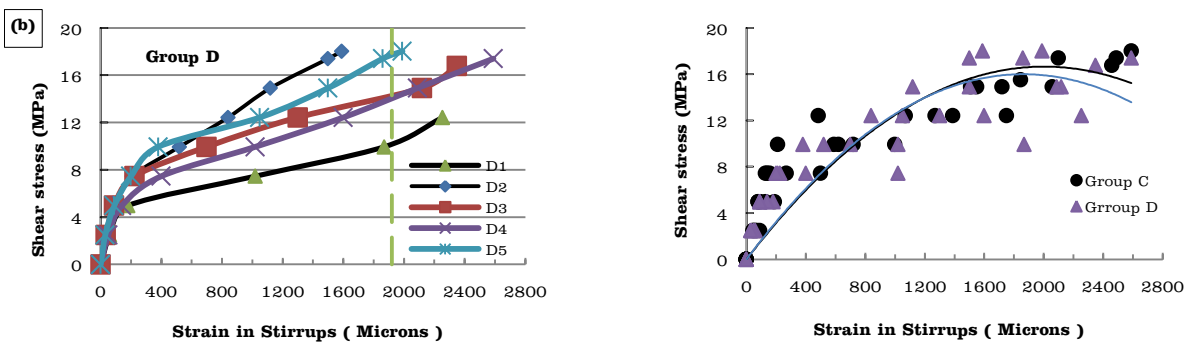

Fig. 14: Shear stress –strain in stirrups relationships : (a) Group C ; (b) Group D.
(Source: Researcher)

Fig. 15: Shear stress – Strain in Stirrups relationship for Group C and Group D.
(Source: Researcher)

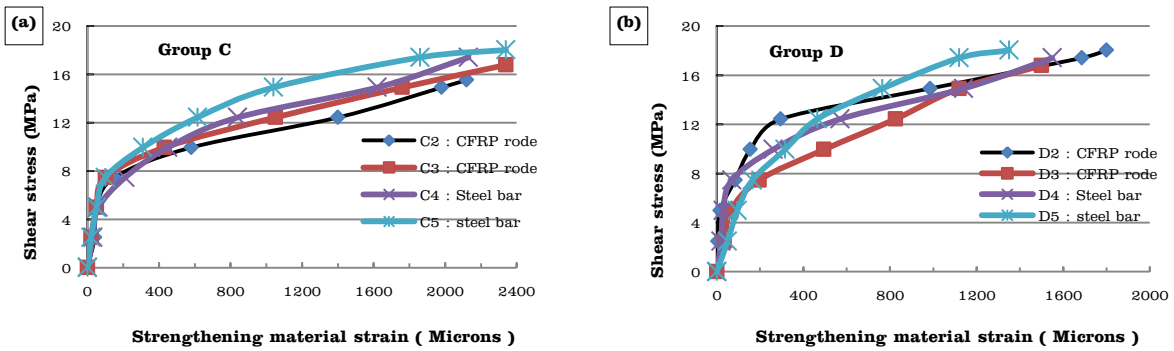

Fig. 16: Shear stress – Strengthening materials strain relationships: (a) Group C ; (b) Group D. (Source: Researcher)

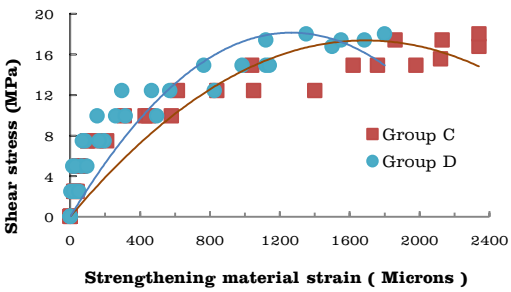

Fig. 17: Shear stress – Strengthening materials strain relationship for Group C and Group D. (Source: Researcher)

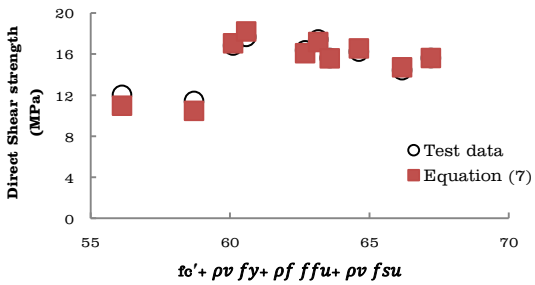

Fig. 18: Relationship between shear strength and predicted equation values. (Source: Researcher)

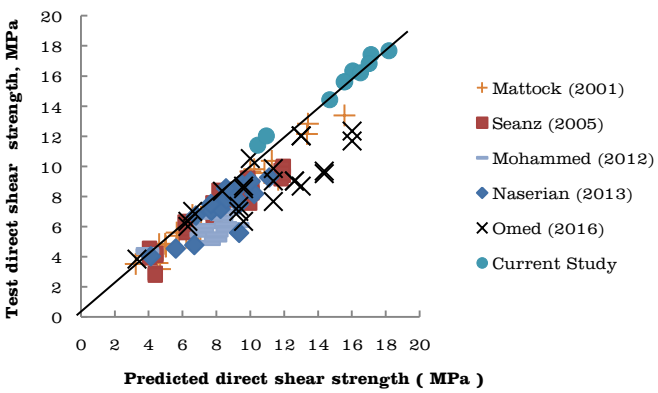

Fig. 19: Comparison of test and predicted results. (Source: Researcher)